

# Antiproton Production and Cooling at the Tevatron

F. Bieniosek, M. Church, G. Jackson, S. O'Day, R. Pasquinelli

Fermilab\*, Batavia, IL, USA

Plans to upgrade the Fermilab Antiproton Source in preparation for Main Injector running are currently being implemented. A permanent magnet storage ring has been proposed to expand Fermilab's  $\bar{p}$  storage capacity while adding the ability to recover stored Tevatron  $\bar{p}$ 's. A beam sweeping system is under development to sweep the beam as it strikes the production target to insure that the target survives without compromising the  $\bar{p}$  yield per proton on target. Changes are being made to the lithium collection lens just downstream of the target which will permit higher gradient operation. The Debuncher ring transverse stochastic cooling upgrade has begun and includes plunging pickups and kickers operating at 4° K and a ramped  $\eta$  which is .006 during bunch rotation and .009 during cooling. The Accumulator ring stacktail momentum system bandwidth will be expanded from 1-2 GHz to 2-4 GHz to handle a higher  $\bar{p}$  flux. The  $\eta$  of this machine will be changed from -.023 to -.012 to accommodate the new 2-4 GHz stacktail bandwidth while avoiding Schottky band overlap.

## 1 INTRODUCTION

The Fermilab Antiproton Source has had unprecedented success during Collider Run I[1]. The modifications necessary to improve further during Collider Run II with the Main Injector will be described in this paper.

Figure 1 shows the target station, the Debuncher ring, the Accumulator ring and the connecting transfer lines. The Main Injector replaces the Main Ring in Run II and provides the 8cm long Ni production target with a 1.6  $\mu$ s long batch of  $5 \times 10^{12}$  protons every 1.47 seconds. Upstream sweep magnets sweep the protons in a circle on the target. A 900 T/m lithium lens collects and focuses the 8.9 GeV/c secondaries emerging from the target within a 35 milliradian cone. These secondaries are unswept by downstream sweep magnets and then are transported to the 500m circumference Debuncher ring. After the 53 MHz bunch rotation( at  $\eta=.006$ ), longitudinal and transverse stochastic cooling( at  $\eta=.009$ ) is applied before the  $\bar{p}$ 's are transferred into the 475 m Accumulator ring. The beam is stochastically cooled and stacked for 1 hour in the upgraded Accumulator until roughly 20 mA has been collected. The  $\bar{p}$ 's are then cooled for high efficiency extraction to the Main Injector/Recycler[2]. Hourly transfers continue until  $300 \times 10^{10}$   $\bar{p}$ 's are stored in the Recycler( stacked plus

recycled beam). After that, extraction for collider luminosity begins.

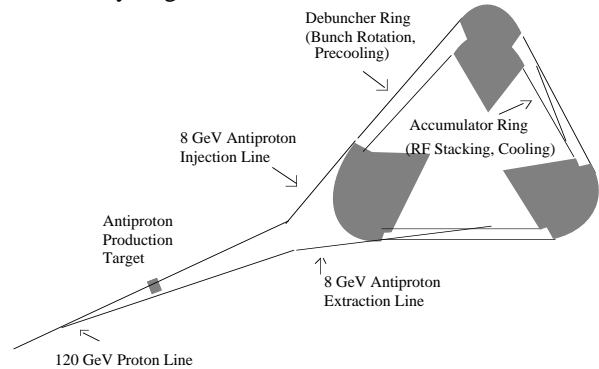


Figure 1. Antiproton Source Layout.

## 2 TARGETRY AND COLLECTION

### 2.1 Proton Beam Sweeping

The efficiency of collecting antiprotons from the target rises as the size of the proton beam spot on the target is reduced[3]. At the same time however, the peak energy deposition on target rises. The 800 J/g energy density estimated for Run I is close to the melting point of nickel (about 1000 J/g) and deleterious effects to the target have been observed[4]. In order to achieve a peak energy density below present levels under Main Injector conditions, the spot size will have to be increased from .19mm to at least 0.30 mm. The alternative is to sweep the beam on the target[5,6]. Reducing the spot size to the smallest attainable size (.10-.15 mm) leads to a 15-20% increase in yield while decreasing the energy deposition density.

The beam sweeping scheme currently under development utilizes two upstream sweep magnets driven in quadrature by a pair of 625 kHz sinusoidal current supplies to trace a circular pattern of .33 mm radius on the target in 1.6  $\mu$ s with the 120 GeV proton beam pulse. Two downstream magnets redirect the 8 GeV antiprotons exiting the collection lens such that they are parallel to the AP2 transport line. The sweeping radius is much smaller than the 2 cm diameter of the lithium collection lens and the aperture of the AP2 beamline. Approximately 6 kA will be required in the single-field sweep magnets to provide the deflecting field over a 3-cm aperture, and the inductive voltage drop will be about 6 kV.

An air gap is used since the beam is already transported through air from upstream of the target to

\* Operated by the Universities Research Association under contract with the U.S. Department of Energy

downstream of the pulsed magnet. A magnetic core surrounding the conductors provides a return path for the magnetic field. Ionization of the air by the particle shower downstream of the target will increase the conductivity of the air between the conductor plates. Electrical losses through the ionized-air path have been determined by measuring leakage current between two conductors placed parallel to the beam path with a voltage drop of up to 16 kV. The current drain is 100 A in agreement with CASIM calculations and a simple plasma model of the air gap.

## 2.2 Li Lens Improvements

The collection lens [7] focuses the 8.9 GeV/c secondaries emerging from the target. The current-carrying lithium portion has a diameter of 2 cm and a length of 15 cm. The front-face of the lens resides 20 cm from the target center. The lithium is encased in a cylindrical water-cooled Ti-6Al-4V jacket. Fermilab lithium lenses of recent design have survived over 7 million pulses at a lens gradient of about 740 T/m (500kA peak lens current). The goal is reliable operation at 900 T/m. Measurements of yield vs. gradient [8] show that this will give an 18% increase in yield compared to 740 T/m.

Raising the field gradient of the lens reduces the focal length and allows the lens to intercept and focus more particles. Unfortunately, higher current results in more Joule heating and thermal stress on the Ti jacket. Small increases in repetitive stress in the Ti-6Al-4V cylinder (which acts as both a cooling jacket and a pressure vessel) lead to a much shorter fatigue life of the metal. Thus operation at even 5% greater field gradient has not proven possible beyond 1-2 million pulses. Several mechanical and manufacturing improvements in the design of the lens are expected to further improve reliability and field strength. The principal reduction in Ti jacket stress which will enable lithium lenses to survive at high gradient is a lithium preload reduction.

The preload serves to insure that the lithium cylinder maintains its shape at mid-pulse, when significant magnetic pinch forces are present. The preload is achieved during the filling process when lithium is pumped under pressure into the evacuated titanium vessel. Lower preload leads to lower operating stresses; a small stress decrease on the titanium cooling jacket should result in a great increase in the life of the lens for a given field gradient. A recent analysis using ANSYS [9] shows that it is possible to lower the preload pressure in the lithium by at least 15% for cold-start operation at 20 °C. At steady state, the lens is at 65°C and the additional thermal stress on the titanium is approximately the same as the stress due to preload. Thus, at steady state almost no preload is needed. If one could reduce the lithium preload from 2300 psi to 500 psi, then the lens would be able to operate at 1000 T/m without deformation of the lithium cylinder.

A lens with a preload of 1950 psi is currently being built for 900 T/m operation. This lens will be filled with 99% isotopically pure  ${}^7\text{Li}$  to eliminate the helium and tritium formed in the reaction between  ${}^6\text{Li}$  and thermal neutrons. Without this improvement, the pressure of the contained gas could limit the lifetime of the lens under an intense beam environment.

Fermilab has also recently had discussions with BINP on the development of a 13T/m liquid lithium lens [10]. We hope to understand the potential of such a device before the beginning of Run II.

## 2.3 Debuncher/Lens Matching

The measured transverse aperture of the Debuncher ring is  $240 \times 240 \pi$  mm-mr (normalized 95% emittances). The phase space of particles at the second lithium lens focal plane is  $290 \times 290 \pi$  mm-mr. The measured emittance of the secondaries coming into the Debuncher is  $160 \times 160 \pi$  mm-mr. Efforts to understand the mismatch in the beamline connecting the target and Debuncher ring have been successful and the upgrade of this beamline should produce a 50% gain in antiproton yield per proton [11].

# 3 DEBUNCHER RING COOLING UPGRADE

## 3.1 The Ramped Lattice

Each pulse of beam is cooled in all 3 dimensions in the Debuncher during the entire 2.4+ seconds of the production cycle. There are 128 LN<sub>2</sub> cooled pickup pairs and 128 kicker pairs for each transverse system. Momentum cooling is done by the "filter method" using the sum mode signals from the transverse electrodes, and notch filters are additionally used in the transverse systems to minimize thermal noise power. All 3 systems operate in the 2-4 GHz frequency range [12]. After bunch rotation, the momentum width (95% full width) is cooled from .30% to .17%. The transverse emittances are cooled from  $160 \pi$ -mm-mrad to  $33 \pi$ -mm-mrad.

The transverse emittance cooling rate is given by [13]

$$-\frac{1}{\varepsilon_{\perp}} \frac{d\varepsilon_{\perp}}{dt} = F_0 \sum_l \left\{ g_l T_l - \frac{N}{2} |g_l T_l|^2 (M_l + U_l) \right\}$$

where for simplicity we have neglected imaginary parts due to "bad mixing", non-optimum pickup to kicker betatron phase advance, and microwave signal processing hardware. The summation is over Schottky bands and the quantities within the summation are averaged over beam frequencies in each Schottky band. The time evolution of the emittances has been calculated and compared to the measured emittance cooling rate.

Currently the system is running substantially below the optimum gain. Optimum gain at the center of the beam distribution is given by

$$g_{opt,l} = \frac{1}{\frac{M_{peak,l}}{2} + U_l}. \text{ At midband, the mixing } M_l \text{ is 6}$$

at the beginning of the cycle, increasing to 11 at the end of the cycle;  $U_l$  is 10 at the beginning of the cycle, increasing to 40 at the end of the cycle. In addition, the maximum cooling rate is limited by the thermal power ( $U_l$ ).

We are prevented from increasing the gain by the power limitation of the kicker tanks -- these tanks are limited to about 1200 W per system by the power handling capability of the terminating resistors, solder joints, vacuum feedthroughs, and microwave hybrids. (At 1200W 95% of the power at the kickers is thermal power.) During Run II, the power handling capabilities of the kicker tanks will be increased from 1200W/system to 2000W/system by increasing the water cooling, improving the microwave hybrids, replacing the 3 dimensional loop electrodes with planar arrays, and using higher wattage terminating resistors.

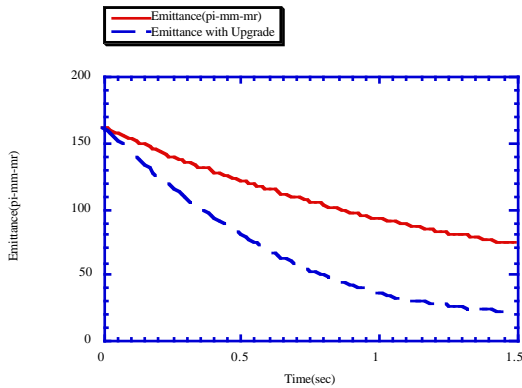


Figure 2. Debuncher cooling rates.

The power handling upgrade mentioned is unfortunately insufficient since the cycle time and the intensity per pulse will be 1.6 times greater than in Run 1B. To address this, several steps will be taken. First, the noise power will be reduced by a factor of 5. This is accomplished by cooling the pickup arrays, terminating resistors, and combiner networks to 5°K with liquid helium and by replacing the 40°K preamplifier with a 20°K preamplifier. Second, the signal/noise ratio will be increased by using "plunged" pickup and kicker arrays. Since the sensitivity (gain) is inversely proportional to the electrode separation, decreasing the separation as the beam shrinks transversely during the cooling cycle will increase the overall gain and increase the signal/noise ratio with no increase in thermal power (this technology has been in use for years at CERN's ACOL ring). Finally, the Debuncher lattice will be ramped during the cooling cycle.  $\eta$  changes from .006 during bunch rotation to .009 during

the cooling cycle. This will decrease  $M_l$  by a factor of 1.5 for most of the cooling cycle. This has already been implemented during studies and a successful ramp from .006 to .008 has been shown to improve the stacking rate[14].

The above upgrades will utilize all of the existing 2-4 GHz middle level and high level microwave hardware while the pickup and kicker tanks will be completely redesigned. Figure 2 shows the predicted transverse cooling rates under various combinations of the above upgrades assuming  $12.2 \times 10^7$  antiprotons/pulse and a 1.5 second cycle time. The upgrades proposed are seen to easily achieve the desired  $48\pi$  mm-mr emittance on transfer to the Accumulator.

## 4 STACKTAIL MOMENTUM UPGRADE FOR THE ACCUMULATOR RING

### 4.1 2-4 GHz Stacktail Momentum Cooling

During Collider Run II, the antiproton flux will increase from  $2.0 \times 10^7$  to  $8.1 \times 10^7$  per second. With the introduction of the Recycler ring, the maximum antiproton stack size will be reduced from  $200 \times 10^{10}$  to  $20 \times 10^{10}$  and the dynamic range of the beam longitudinal density in the Accumulator will be reduced from  $4 \times 10^4$  to  $4 \times 10^3$ . Correspondingly, the core density before extraction will be reduced from  $16.1 \times 10^4$  to  $5.6 \times 10^4$  eV<sup>-1</sup> (@  $10\pi$  mm-mr normalized emittances). Nonetheless, the current stacktail cooling system in the Accumulator will be inadequate to meet these conditions. We propose to increase the bandwidth of the stacktail cooling system from 1-2 GHz to 2-4 GHz and to decrease  $\eta$  by a factor of two from -.023 to -.012. The bandwidth change will supply the necessary cooling force to handle the increased flux and the  $\eta$  change will avoid Schottky band overlap, which causes excessive beam heating, and will allow the use of conventional notch filters for gain shaping. In general aspects, the system will be similar to the current system.

The maximum attainable flux in a "perfect" single octave bandwidth stacking system is given by [15]  $\phi_{max} = 1.4 W^2 E_d \eta / p F_0$  where  $W$  is the bandwidth,  $1/E_d$  is the exponential gain slope,  $p$  is beam momentum, and  $F_0$  is the revolution frequency. This equation neglects thermal noise, signal suppression, phase variations across the Schottky band, and the effects of periodic beam injection, but indicates that doubling the bandwidth and halving  $\eta$  will double the maximum attainable flux.  $E_d$  is 10 MeV, so that we have for the current stacktail system  $\phi_{max} = 21 \times 10^{10}$ /hour. Factors which will further reduce the stacking rate, in addition to the factors mentioned above, are intrabeam scattering,

intermodulation distortion in TWTs, gain and phase variations across the microwave band, and crosstalk from transverse cooling systems. We have attempted to include all of these effects (crudely in some cases) so that the current performance of the Accumulator cooling systems is well predicted by the stochastic cooling simulation.

We have used a "macroparticle" simulation[16] to model the behavior of the current Accumulator stacktail and core momentum cooling systems. The results of open loop beam transfer function measurements on the present momentum systems have been included. Transverse heating of the core by imperfections in the longitudinal systems is included as well. With both longitudinal and transverse heating terms added, the stochastic cooling simulation was run on the current system at a flux of  $13 \times 10^{10}$ /hour for 1 hour with no beam losses. During a Run I experiment, a stacking rate of 12.2 mA/hr was achieved stacking protons.

Simulations have been run using the following expected upgrade parameters:

- 1) 2-4 GHz stacktail system, and 4-8 GHz core momentum cooling;
- 2) gain profile is identical to the measured gain profile of the current system, but gain is scaled;
- 3) 125°K real thermal noise plus 235°K added thermal noise (the effect of this noise scales with gain squared);
- 4) no transverse heating;
- 5) flux of  $24 \times 10^{10}$  @ 1 pulse/1.5 sec @ input ( $\Delta p/p$ )<sub>95%</sub> = .0017;
- 6) 30 minutes of stacking.

There is an optimum gain (figure 3) which produces the minimum ( $\Delta p/p$ ) at the core after 30 minutes of stacking -- systems with gains below this optimum do not push beam into the core fast enough; systems with gains above the optimum heat the core excessively.

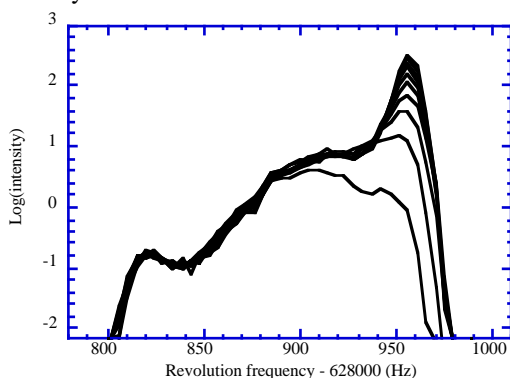


Figure 3. Accumulator stacktail in 3 minute intervals.

#### 4.2 A Larger $\gamma_t$ Lattice

Using the Methodical Accelerator Design (MAD) simulation code, a strategy for raising  $\gamma_t$  in the

Accumulator ring has been developed which will have minimal impact on tunes, cooling system phase advances and lattice parameters. The dispersion will be similar to the present Accumulator with a slightly more negative dispersion in non-critical parts of the ring to accomplish the change in  $\gamma_t$ .

The Accumulator is divided into 6 sectors, each containing fourteen quadrupole magnets. The symmetry is three-fold with each of the six sectors being a reflection of the adjacent sector. Changes to existing quadrupole currents and the replacement of one large quadrupole in each sector will enable  $\gamma_t$  to be raised from 5.41 to 6.58 (corresponding to an  $\eta$  change from -.023 to -.0119). To facilitate the current changes, 6 shunts will have to be installed in each sector for a total of 36 new shunts.

## 5 THE RECYCLER

### 5.1 Introduction to the Recycler

The Recycler is a fixed 8 GeV kinetic energy storage ring which will reside in the Main Injector. This project was first proposed less than two years ago and is presently being considered for inclusion in the Main Injector project. The cost effectiveness and simplicity of producing a storage ring with the exclusive use of permanent magnets is expected to result in this ring being ready at the beginning of Main Injector commissioning.

As proton intensities, stack size requirements and duty cycle frequencies have increased, the ability of the Antiproton Source to stack antiprotons efficiently has been challenged. It is clear that additional antiproton capacity is necessary in order to exceed Main Injector goals. This new ring will satisfy the need for extra antiproton storage capacity and hopefully provide some additional benefits.

The name of this machine is derived from the plan to recover antiprotons from one Tevatron store for use in a later store. The Recycler may drop fewer stacks since it does not depend on external power or regulation to maintain a constant magnetic field. The Recycler can be more efficient at large stacks since it is required to stack over a more limited dynamic range than the existing Accumulator. In turn, the Accumulator then only needs to stack where it stacks best- from 0 to 20 mA. The gain from having recycled antiprotons from a previous Tevatron store is reflected in the total number of antiprotons available for collider operations and in the luminosity. The number of stored antiprotons rises from  $144 \times 10^{10}$  to  $288 \times 10^{10}$  with the introduction of the Recycler. The achievable integrated luminosity (per store) rises from 2.9 to  $3.4 \text{ pb}^{-1}$  as well.

### 5.2 Recycler Lattice and Components

The Recycler ring lattice is basically a clone of the Main Injector lattice in which there are two 4m long 1.5

kG gradient magnets in each arc half cell. The ring has the same circumference(3320m) as the Main Injector and resides 7 feet above it. Special considerations in the MI-60 rf straight section force the Recycler to swing radially outward by 18 inches. Eight special quadrupoles have been placed around the dispersion suppressor elements to accomplish this bypass while matching the lattice functions.

There are 416 magnets which come in 3 varieties. Each cell structure provides  $90^\circ$  betatron phase advance. The normal FODO arc cells consist of four 4.2m permanent gradient magnets. Dispersion suppressor cells are made up of four 2.8m long permanent gradient magnets. Straight section cells consist of four .5m long permanent magnet quadrupoles. The lattice design leads naturally to a tune of  $(\nu_x, \nu_y)=(26.225, 26.215)$ . Tracking studies indicate that the Recycler can easily store a  $30\pi$  mm-mrad beam whose momentum spread is within .1% of 8.9 GeV.

### 5.3 Recycling Antiprotons

At the end of a store, the protons will be scraped or aborted. The electrostatic separators will be turned off to increase the antiproton aperture. Regulated ramps will decelerate the beam to 150 GeV at 16 GeV/sec. The Main Injector will be loaded via nine transfers of 4 bunches each. The deceleration will continue using 53 MHz rf at 4 MV. At 25 GeV, 2.5MHz rf at 60kV will be turned on to bring the beam to 8 GeV( transition is crossed).

The Recycler is ready for new recycled beam after the cooled beam already in the Recycler has been longitudinally compressed. Typically, there will be 54 eV-sec of cooled beam compressed so that it occupies 1/4 of the ring( with an rms energy spread of 4.8 MeV).Barrier buckets protect the "old" beam while new beam is being injected with 2.5 MHz 1.6kV bucket to bucket transfers. Nine transfers occur with each new batch being merged with previous transfers after it arrives using rf manipulation. The cooled beam will be transferred to the Tevatron for the next store before the newly recycled beam is allowed to expand to fill the Recycler ring.

### 5.4 Antiproton Stacking

Approximately  $20 \times 10^{10}$  antiprotons will be injected into the Recycler once per hour. The transverse invariant 95% emittances will be  $10 \pi$  mm-mr in each plane. The longitudinal emittance of each transfer from the Accumulator will be about 9 eV-s. It is expected that six more transfers from the Accumulator will occur before extraction to the Tevatron. The core emittance of the  $288 \times 10^{10}$  antiprotons(  $140 \times 10^{10}$  from the Accumulator and  $148 \times 10^{10}$  antiprotons from recycling) is expected to be 55 eV-s with a density of  $5.3 \times 10^{10}$  antiprotons/eV-s. This prediction is based on an intrabeam scattering and stochastic cooling model[2]. It should be noted that only stochastic cooling will be in place during Recycler

commissioning. Electron beam cooling is presently in a research and development phase and will later improve the longitudinal cooling rate.

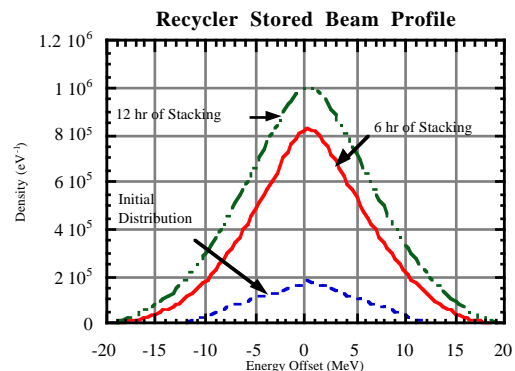


Figure 4. Stacking in the Recycler.

After the consideration of various alternatives, it has tentatively been decided that the stochastic momentum cooling will come from a .5-2 GHz filter cooling system. A simulation of this system after 12 hours is shown in figure 4. Note that Palmer cooling( as in the present Fermilab Accumulator) cannot be used because the present lattice does not include a suitable low  $\beta$  high dispersion section. A 2-4 GHz filter cooling system was also investigated, but the intrabeam scattering forces the beam to lie where the real part of the gain function passes through zero degrees. Particle loss resulted.

2-4 GHz bandwidth horizontal and vertical betatron cooling have been studied. The transverse systems appear to be low power and should need only one TWT per plane. System parameter optimization continues.

## REFERENCES

- [1] V.Bharadwaj et al.,FERMILAB-TM-1970(1996).
- [2] Fermilab,*Fermilab Recycler Ring TDR*, Batavia,IL(1996).
- [3] S.O'Day and F.Bieniosek, Proc. 4th EPAC,p.2438-2441(1994).
- [4] S.O'Day and F.Bieniosek,Proc. 1993 U.S. Part. Acc. Conf.,p.3096-3098(1993).
- [5] F.Bieniosek, FERMILAB-TM-1857(1993).
- [6] F.Bieniosek, K.Anderson, K. Fullett, Proc. 1995 U.S. Part.Acc. Conf., Dallas,Texas.
- [7] G.Dugan et al., IEEE Trans. Nucl.Sci.30:3660-3662(1983).
- [8] S.O'Day and F.Bieniosek,Nucl.Inst.Meth.A343, p.343-350(1994).
- [9] S.O'Day and K.Anderson, Proc. 1995 U.S. Part.Acc. Conf., Dallas,Texas.
- [10] B.Bayoanov et al., IYF-84-168.
- [11] Fermilab,*Fermilab Main Injector Handbook*, Batavia,IL(1995).
- [12] Fermilab,*Design Report for the Tevatron I Project*, Batavia,IL(1984).
- [13] D. Mohl, CERN 87-03 V2:453-533(1987).
- [14] D. Olivieri, U.Mass. Ph.D. Thesis(1996).
- [15] J. Bisognano and C. Leeman,AIP Conf. Proc. #87,Fermilab Summer School on Acc. Phys.(1981).
- [16] A. Gerasimov, Fermilab-Pub-94/376(1994).